International Journal of Engineering Research and General Science Volume 3, Issue 4, July-August, 2015
ISSN 2091-2730

An experimental and numerical study on laser percussion drilling of 316-Stainless Steel

Anita Pritam, , Dr. R.R. Dash, Dr. R.K. Mallik

Ph.D. Scholar, CET, Bhubaneswar, Email: anitapritam@gmail.com, Contact no: 9437298202

Abstract— A major challenge in laser percussion drilling of steel is to enhance the material removal rate by optimizing the process parameter. In this paper, an experimental and numerical study on laser percussion drilling was carried out. A two-dimension (2D) axisymmetric finite element (FE) model for simulation of temperature field and proceeding of hole formation during percussion drilling was developed. The FE model was validated by the corresponding experiment. Furthermore, a theoretical model for evaluation of temperature fields at melt front was presented. The effects of laser peak power, pulse frequency, pulse width on MRR were investigated by the developed models and experiments, in which the simulated results were in good agreement with the experiments. Based on the experimental and numerical study, the process parameters were optimized and a drilled-hole with low taper and low spatter deposition was obtained using a 2.5kW CO_2 laser.

Keywords— FEM, Simulation, Laser percussion drilling, MRR, Temperature Profile,

INTRODUCTION

Nowadays, laser drilling is an industrial process used for cutting all types of materials. Laser drilling has wide application in the field of automotive industry [1], aeronautic sectors, steam turbine power plants, nuclear reactors etc. Continuous-wave CW CO_2 laser is most often used for this application. The assist gas type and pressure have strong influence on the quality of produced cuts. The assist gas is responsible for removing the molten metal from the cut kerfs, and it protects laser optics from beginning damaged by the resulting ejected spatters [2]. The aim of article is numerical simulation laser cutting process specifically to find appropriate methodology of computer modeling. The numerical simulation of laser cutting process was carried out using the solution of an inverse heat transfer problem [3]. 2D simulation models have been created with emphasis on the comparison of calculated and measured temperatures. For numerical simulation of laser cutting process was used finite element method (FEM). FEM for discrete areas can be characterized as continuous computer-oriented method for solving differential equations [4]. For numerical simulation, the software used is ANSYS. ANSYS was used for creation of 2 D model of laser drilling process with SHELL elements. Shell and Solid simulation models are supported with obtained data from real experiment implemented in IIT,Guwahati. The main aim is to help elucidate simulation model creation of laser drilling process.

METHODOLOGY FOR SIMULATION MODEL CREATION

2D SHELL model

Used element type for 2D SHELL model was SHELL 131 with added material thickness. The base of methodology for input of heat load to the cutting area is the theory of heat transfer and boundary condition definition. Heat load for SHELL model was implemented as an input surface temperature into gap nodes. This is first-type (Dirichlet´s boundary condition of first kind) [°C]. The surface temperature of drilled material may appear as a constant or may depend on the coordinates (distributions function), from time. It is an indirect method. Simulation model was created as plane symmetrical. Half dimensions of the sample were used. Dimensions of sample were $0.025\times0.025\times0.005m^3$. The plane of symmetry is central plane of the cut also. The distance of thermocouples from central plane of the cut was 0.002 and 0.0054 m. Distance between them was 0.02 m. Direction of movement laser beam was simulated along central plane of the drilled hole point. The temperature measured with thermocouples was recorded [5].

FULL MODEL

Laser drilling was simulated by the model which was full of metal. After moving of heat source along symmetrical plane of the cut, liquid metal remained in laser gap. Heat source movement was simulated sequentially. First, were selected elements with laser gap dimensions. Subsequently selected elements were heat loaded. Heat load was temperature which varies depending on the time of laser beam movement. Gradually were selected and loaded all elements along central plane of the cut.

AIR MODEL

AIR model gradually change metal elements onto air behind laser beam movement. All elements along symmetrical plane of the cut were selected and loaded by defined load steps. Function for gradually changing material into air after the movement laser beam was added. Changing was realized with change material properties. Material properties for steel and air were used [6].

KILLING MODEL

Model was created for deactivated (killing) elements [7] after the heat source movement elements were consequence killed. Elements were gradually removed from laser gap. All elements along symmetrical plane were gradually selected, loaded and killed.

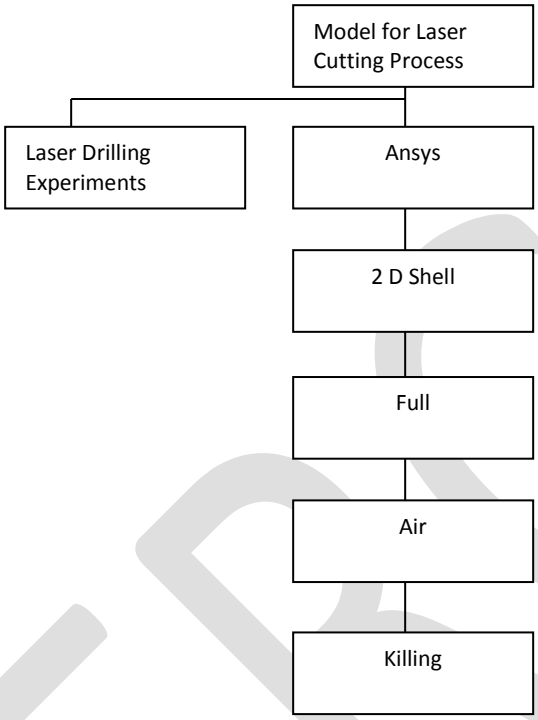

Fig. 1 Process of creation computer modeling

FEM-BASED THERMAL MODELLING

In LBPD, absorption of laser energy from a high intensity laser beam takes place and it is converted into thermal energy to raise the temperature within the laser-irradiated zone. The hole profile as well as the temperature distribution inside the workpiece change continuously with respect to co-ordinate axes fixed at the laser beam; therefore, LBPD is considered as a non-steady process. The nature of thermo–optic interactions between the laser beam and the work-piece play a crucial role in determining the efficiency of LBPD. Therefore, several aspects, like (i) temperature dependent thermal properties (ii) temperature dependent optical properties (absorptive) and (iii) phase change phenomena have been incorporated in the thermal model to evaluate the temperature distribution during LBPD.

Due to the complex nature of the LBPD process, a number of assumptions have been made in deriving the thermal model.

1. The zone of influence of pulsed laser beam in the sheet form of the work piece is considered to be axisymmetric, i.e., $\frac{dT}{d\theta} = 0$.
2. The sheet material is homogeneous and isotropic in nature.
3. On-time of pulsed laser is considered to be much shorter than the pulse-off time, and therefore plasma generation does not take place in the laser-drilled hole.
4. The evaporated material is transparent and does not interfere with the incoming laser beam.
5. The metal vapor is optically thin so that its absorption of the high-energy beam is negligible.
6. Gaussian spatial distribution of the laser heat flux is assumed due to the smooth drop of irradiance from the beam center towards the radial direction.
7. Since in the LBPD process, it is very difficult to track the solid– liquid and liquid–vapor interfaces, it is assumed that all the molten material has been removed from the hole once the melting takes place.
8. Multiple reflections of the laser irradiation within the hole are neglected.

GOVERNING EQUATION

Considering the axisymmetric model the differential equation in conduction mode of heat transfer neglecting internal heat generation for cylindrical co-ordinate system can be given by Eq. (1) [8].

$$\rho C_p\left[\frac{\partial T}{\partial t}\right]=\left[\frac{1}{r}\frac{\partial}{\partial r}\left(K\frac{\partial T}{\partial r}\right)+\frac{\partial}{\partial Z}\left(K\frac{\partial T}{\partial Z}\right)\right] \quad (1)$$

Where ρ is density, C_p is specific heat, *K* is thermal conductivity of the work piece, T is temperature, t is the time and r & Z are coordinates of the work piece.

HEAT DISTRUBUTION

The heat generated by the laser beam creates a plasma channel, which resulting the temperature rise on the work piece surface. For LASER process the plasma distribution on the work piece surface can be assumed either as uniform disk source or Gaussian heat distribution [6-9,14,15]. For the present analysis Gaussian distribution of heat flux is assumed on the work piece surface since it is more realistic and accurate than the uniform disc heat source [14]. A schematic diagram of thermal model with the boundary conditions is shown in the Fig. 2.

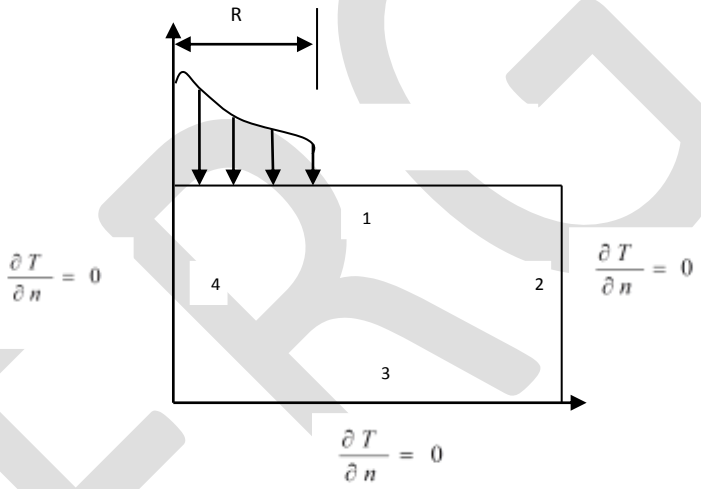

Fig.2 Axisymmetric boundary conditions

BOUNDARY CONDITIONS

Since the model is axisymmetric in nature therefore one half of the work piece is considered for analysis. The work piece domain along with applied boundary conditions is shown in Fig. 2. A Gaussian distribution of heat flux was applied on the work piece surface and the flux was applied on boundary 1 up to radius R same as of the laser beam diameter. The effect of heat transfer is considered to be negligible on the surfaces 2 & 3 since they are far from the heat source location. For boundary 4, heat transfer is zero since an axis of symmetry model is assumed. Applied boundary conditions in mathematical term are given below:

When $0< t < \tau$

$$K\frac{\partial T}{\partial Z}=Q(r), \text{ when } R< r \text{ for boundary 1} \quad (2)$$

$$K\frac{\partial T}{\partial Z}=h_f\left(T-T_0\right), \text{ when } R \geq r \text{ for boundary 1} \quad (3)$$

When $\tau < t < \tau_p$

$$K\frac{\partial T}{\partial Z} = h_f\left(T - T_0\right) \text{ for boundary 1}$$

When $t > 0$

$$K\frac{\partial T}{\partial n} = 0 \text{, at boundary 2, 3 \& 4} \quad (4)$$

Where τ is the pulse width, t_p is the total pulse duration (i.e., on and off time), Q is the amount of heat flux entering the sheet, R is the laser beam radius, h_f is heat transfer coefficient, T_0 is the ambient room temperature, and direction n is outward normal to the boundary surface. Moreover, the absorption coefficient is the inverse of penetration depth (also known as absorption depth). The value of this absorption depth relative to the thickness of irradiated sheet is negligible (for metals) therefore the energy supplied by the laser source can be modelled as a boundary condition whereas in case of non-metals like ceramics this value is not negligible, and hence the laser beam must be modeled as volumetric heat source.

HEAT INPUT

The laser beam is radially symmetric with a Gaussian heat flux profile. Heat flux at a distance 'r' from the center of the laser beam on the surface of the sheet is given by Eq. (5) [9]. The change of laser beam radius with the depth can be evaluated using Eq. (6).

$$Q(r) = A_S\frac{2P_P}{\pi R^2}\exp\left\{\left(\frac{-2r^2}{R^2}\right)\right\}$$

where As is the absorptivity, P_P is the laser peak power, R is the effective beam radius, which varies with the depth of the hole due to defocusing, d is the beam diameter (500 mm), fc is the focal length of lens (50mm), Z_m is the melt depth, and l is the wavelength of the laser beam. The value of P_P can be obtained using Eq. (7).

$$P_p = \frac{Average\ Laser\ power\ (W)X1000}{Repetition\ rate\ (Hz)XPulse\ width\ (ms)}$$

EXPERIMENTAL SETUP AND RESULTS

The experiments have been performed on ORION - 3015 CO_2 laser cutting machine using nitrogen as an assistant gas for cleaning the extra material after machining (flushing) (Figure 2). ORION-3015 is carbon dioxide (CO_2) laser cutting machine setup having 2.5kW power, wave length of 10.6 µm is latest design to provide an intelligent and cost effective solution for laser processing needs. It is controlled by Fanuc CNC control features with 9.5" color screen. CADMAN-L 3D software is used for controlling laser processing set up. The laser cutting machine is available at Indian Institute of Technology Guwahati. The laser machine is supplied by LVD Company (Belgium). Expermints were perfomed on 316-stainless steel specimen having dimensions of $0.2\times0.1\times0.005$ m^3. . The main aim of experiments was to find out the transverse temperature distribution and MRR. Process parameters were used: pressure of assist gas - 13 bar, cutting speed - 0.7 $m.min^{-1}$, nozzle to material distance - 0.8 mm and laser power 2.5 kW. The material property of the specimen is given in table-1. And Figure 3 shows the work piece and machine setup.

MATERIAL PROPERTIES OF 316-STAINLESS STEEL

Table-1

Density, ρ (kg/m^3)	7500
Melting temperature, T_m(K)	1400
Thermal conductivity (W/mK)	29
Heat capacity(J/kgK)	630
Latent heat of vaporization,L_v(J/kg)	$7.6x10^6$
Latent heat of fusion,L_f(J/kg)	$2x10^5$

Fig.3 Experimental Setup

FINITE ELEMENT SIMULATION OF THERMAL MODEL

For the solution of the model of the LASER process commercial ANSYS 11.0 software was used. An axisymmetric model was created. A non-uniformly quadrilateral distributed finite element mesh with elements mapped towards the heat-affected regions was meshed, with a total number of 2640 elements and 2734 nodes with the size of the smallest element is of the order of 0.0015 × 0.0015 cm^2. The approximate temperature-dependent material properties of stainless steel, which are given to ANSYS modeller, are taken from [8]. The governing equation with boundary conditions mentioned above is solved by finite element method to predict the temperature distribution and thermal stress with the heat flux at the laser tip location and the discharge duration as the total time step. First, the whole domain is considered to obtain the temperature profile during the heating cycle. The temperature profile just after the heating period is shown in Fig.3, which depicts four distinct regions signifying the state of the workpiece. Fig.4 and 5 shows typical temperature contour of stainless steel under machining conditions.

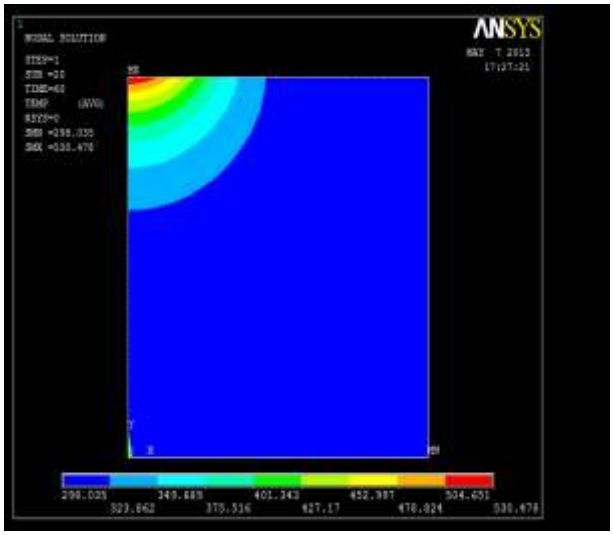

Fig.4 Temperature Profile

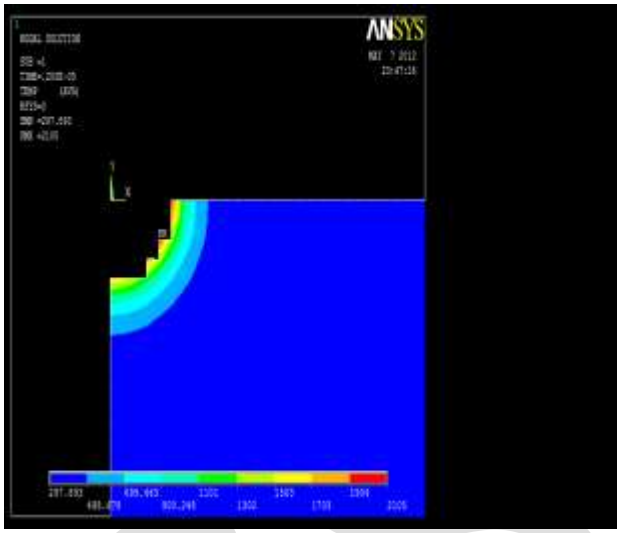

Fig.5 Profile after Melting of Material

SAMPLE CALCULATION FOR MRR FROM SIMULATION RESULT

The dome shaped crater formed on the workpiece after material removal is assumed to be spherical shape. The volume of dome is presented below by Eq. (6).

$$C_v = \frac{1}{6}\pi h\left(3r^2 + h^2\right) \quad (6)$$

Where r is the radius of spherical dome and h is depth of dome.

From geometry:

h = 0.004 m

r = 0.00325 m

The volume of material removal is calculated by calculating the volume of the dome (C_v).

$$C_v = \frac{1}{6}\pi h\left(3r^2 + h^2\right) = 98 \text{ mm}^3$$

For multi discharge machining process the number of Pulse (NOP) during machining is calculated by dividing the total time of machining of the workpiece to pulse duration time.

$$\text{NOP} = \frac{T_{mach}}{T_{on} + T_{off}} = \frac{20}{1000 \times 10^{-3}} = 20$$

Where T_{mach} is the machining time, T_{on} is pulse-on time and T_{off} is pulse-off time.

For multi-discharge machining the MRR is calculated as:

$$\text{MRR} = \frac{C_v \times NOP}{T_{mach}} = \frac{98 \times 20}{20} = 98 \text{ mm}^3/\text{sec}$$

TABLE 2

EXPERIMENTAL DATA OF MRR

T (ms)	F (Hz)	P_p (KW)	T_h (mm)	MRR in (mm^3/sec) Expt.	MRR in (mm^3/sec) FEM
1	10	5	0.7	93	98
1	20	15	1.3	141	151
1	15	10	1	123	120
3	15	15	0.7	154	160
3	10	10	1.3	102	105
3	20	5	1	125	130
5	10	15	1	143	145
5	20	10	0.7	178	190
5	15	5	1.3	113	120

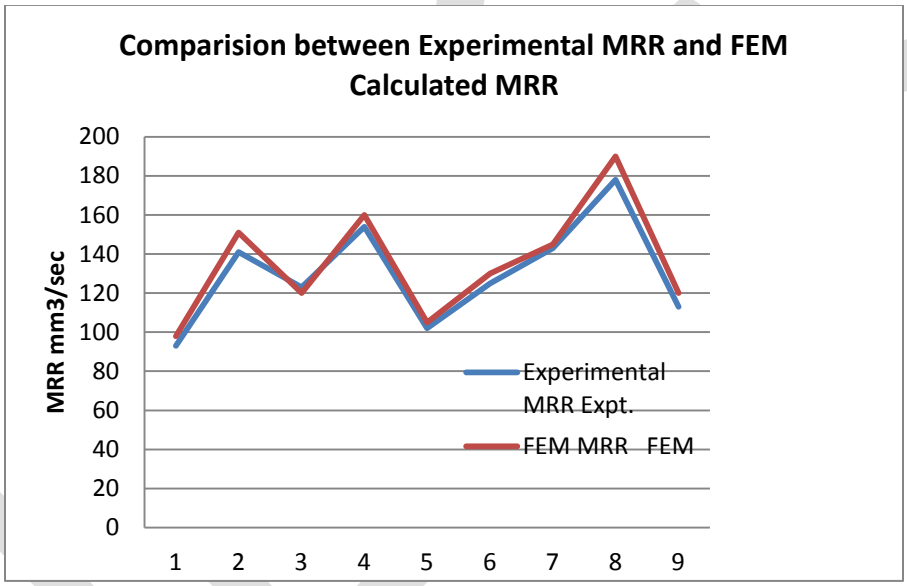

Fig.6 Comparisons between Experimental MRR to the FEM Calculated MRR

RESULT AND DISCUSSION

Taking stainless steel as work piece the results have been obtained. According to Gaussian distribution of heat flux, the heat flux is maximum at the center line, on the top surface of the work piece. Temperature distribution in the work piece has been shown in Fig. 4. From the simulation result it is clear evident that at the center line, on the top surface of the work piece highest temperature generates.

The high temperature rises due to laser beam can easily melt the material and formed a dome in the work piece. This is evident from the temperature distribution after material removal in FEA model as shown in Fig. 5. The volume of metal remove depends on amount of heat energy induced in the material. Therefore the MRR increases with increase in pulse width pulse frequency and peak power.

Fig.6 shows the graphical representation of MRR obtained in FEM model and experimentally. Out of nine no of experiment eight experimental result are almost equal to the predicted MRR obtained by FEM model.

CONCLUSION:

In this paper, CO_2 laser percussion drilling of thick-section (5-mm-thickness) 316 stainless steel was studied. The effects of process parameters (i.e. laser peak power, pulse frequency and pulse width) on MRR were investigated by experiments and numerical simulations. It was found that the MRR increases with increase in pulse width, pulse frequency and peak power at a given thickness. Then the experimental results were compared with FEM model by using ANSYS 11 software which shows a good agreement with experimental result.

REFERENCES:

[1] A Cekic, M Kulenovic, D Begic, and J Bliedtnerb "Investigation of optimum condition in laser cutting of alloy steel 1.4571 using air assist gas" In Proceedings of the 20th International DAAAM Symposium., Vienna, Volume 20, No.1, 1347-1348, . 2009.
[2] H. G. Salem, M. S. Mansour, Y. Badr, and W. A. Abbas, "YAG laser cutting of ultra low carbon steel thin sheets using O2 assist gas" In Journal of materials processing technology, 196, 67-72, 2009.
[3] M. A. Alifanov '' Inverse heat transfer problems' Springer-Verlag, New York London Tokyo, 1994.
[4] S. Benča, 'Computational methods for solving linear FEM task of mechanics' STU, Bratislava, 2006.
[5] E. Babalova, B. Taraba, M Behulova, J Spanielka, "Experimental results for laser cutting of stainless steel plate 5 mm in thickness', In Proceedings of the 22nd DAAAM International World Symposium., Vienna. 675-676, 2011.
[6] F. P. Incropera, D. P. Witt, " Fundamentals of heat and mass transfer", J. Wiley and Sons, New York, 1996.
[7] M. Ghoreishi, B. Nakhjavani "Optimisation of effective factors in geometrical specifications of laser percussion drilled holes", J Mater Process, 196: 303–10, 2008;.
[8] F. P. Incropera, D. P. Dewitt, T. L. Bergman, A. S. Lavine, "Fundamentals of heat and mass transfer", sixth ed. India, New Delhi: Wiley; 2007.
[9] L. Han, F. W.Liou and S Musti, "Thermal behavior and geometry model of melt pool in laser material process", J Heat Transfer, 127:1005–14, 2005.